Available online at www.sciencedirect.com
ScienceDirect
International Journal of Heat and Mass Transfer 51 (2008) 1675–1682
International Journal of HEAT and MASS TRANSFER
www.elsevier.com/locate/ijhmt

Uni-directional heat flux through the horizontal fluid layer with sinusoidal wall temperature at the top or bottom boundaries

Qiu-Wang Wang [a,*], Gang Wang [a,b], Min Zeng [a], Hiroyuki Ozoe [a]

[a] State Key Laboratory of Multiphase Flow in Power Engineering, Xi'an Jiaotong University, Xi'an, Shaanxi 710049, PR China
[b] School of Civil Engineering, Lanzhou University of Technology, Lanzhou 730050, PR China

Received 15 December 2006; received in revised form 23 May 2007
Available online 18 September 2007

Abstract

Infinite horizontal fluid layer is considered between the top and bottom walls. Either top or bottom wall temperature is sinusoidally oscillated in terms of the constant average temperature in an opposing horizontal wall. This is the system with no temperature difference between the top and bottom walls in time-averaged sense, as studied by Kalabin et al. for a square channel. The fluid is Newtonian and Boussinesq approximation is made. The fluid layer of height 1 versus the horizontal width 1 or 4 is adopted and numerical computations are carried out for $Pr = 1$. The time-averaged Nusselt numbers computed both at top and bottom walls give the upward time-averaged heat flux without depending on the temperature oscillation either at the upper or lower walls. This is because the time-dependent convection plumes occur at the almost largest temperature of the bottom wall in comparison to the top wall. The time-averaged heat flux is always positive, i.e., upward, even if the time-averaged temperature difference is zero between the top and bottom walls.

Keywords: Natural convection; Horizontal fluid layer; Sinusoidal wall temperature; Uni-directional heat flux

1. Introduction

The Rayleigh–Benard convection of horizontal fluid layer has been studied for many years. This fluid layer is heated from bottom wall at high temperature and cooled from top wall at low temperature. The heat flux increases from that of conduction to that of convection at the temperature difference greater than that at the critical Rayleigh number of 1708. On the other hand, oscillating temperature boundary condition has been studied for various systems with possible application for meteorological environment, architectural room comfort with oscillatory outside temperature, geothermal systems, etc. Some of them can be found in the literature on the meteorological system primarily [1–4]. More recently resonance natural convection has been studied for sinusoidal temperature oscillation from a wall [5–8]. These are all for the fluid or porous layer heated from one wall and cooled from other wall with temperature oscillation and with temperature difference between two walls in time-averaged sense. However, recently Kalabin et al. [9] studied the convection of fluid in a square enclosure with oscillating temperature on one side wall with the constant average temperature on the opposing side wall. The enclosure is inclined with keeping the third dimension horizontal with presuming two-dimensional flow. They found the time-averaged heat flux is one direction only even if the time-averaged temperature difference between the two opposing side walls is zero. They also found the maximum heat flux at the inclination angle between the wall of oscillating temperature and the vertical gravity direction is 54° at the oscillating frequency of 20π for peak value of the Grashof number $Gr = 2 \times 10^5$ and 3×10^5. They attributed this result to the convection dominance for the time heated from below and conduction dominance for the time cooled from below. Since their result is rather eminent on the control of heat flux in natural convection, we have tried to study further

* Corresponding author. Tel./fax: +86 29 82663502.
E-mail address: wangqw@mail.xjtu.edu.cn (Q.-W. Wang).

0017-9310/$ - see front matter © 2007 Elsevier Ltd. All rights reserved.
doi:10.1016/j.ijheatmasstransfer.2007.07.030

Nomenclature

f	dimensionless oscillation frequency, $\omega h^2/v$
Gr	Grashof number, $g\beta T_1 h^3/v^2$
h	distance between the horizontal two walls, m
k	thermal conductivity, W/(m K)
l	width of a roll cell area, m
n	internal iteration number
Nu_L	local Nusselt number, Eq. (7)
Nu_{bottom}	average Nusselt number computed over a bottom wall, Eq. (8)
Nu_{left}	average Nu computed over a left-hand side wall
Nu_{right}	average Nu computed over a right-hand side wall
Nu_{top}	average Nu computed over a top wall, Eq. (8)
$\overline{Nu}$	time-averaged Nusselt number, Eq. (9)
p_0	a static state pressure, N/m^2
p'	perturbed pressure from p_0, N/m^2
P	dimensionless pressure, $p'h^2/(\rho v^2)$
Pr	Prandtl number, v/α
T_0	constant average temperature, K
T_1	temperature amplitude in oscillation, K
$\mathbf{U}$	velocity vector
U, V	dimensionless velocity components along X- and Y-axes, respectively
u, v	velocity components along x- and y-axes, respectively, m/s
X, Y	dimensionless Cartesian coordinates, $(x, y)/h$
x, y	Cartesian coordinates, m

Greek symbols

α	thermal diffusivity of fluid, m^2/s
β	volumetric coefficient of expansion, 1/K
ε	convergence criterion constant
θ	dimensionless temperature, $(T - T_0)/T_1$
v	kinematic viscosity of fluid, m^2/s
ρ	density of fluid, kg/m^3
τ	dimensionless time, tv/h^2
τ_p	dimensionless period of oscillation
ω	oscillation frequency, 1/s

Superscript

—	time-averaged value

on this issue for a classical Rayleigh–Benard type configuration as reported herein.

The oscillatory temperature on the bottom wall may be one of the models for the oscillating temperature of outside environment in comparison to the room temperature. Then we would like to study the simplest system of the temperature oscillation of the bottom wall in contrast to the constant temperature top wall in the time-averaged sense, or vice versa.

2. Model systems

Fig. 1 shows the schematics of the systems considered herein. Fig. 1(a) shows an infinite horizontal fluid layer in which two-dimensional roll cell is considered with height h and width l. In the present report, we studied both $l = h$ and $l = 4h$. Fig. 1(b) shows thermal boundary condition of Case 1 for which the top wall is kept at oscillatory temperature $T_0 + T_1 \sin \omega t$ ($\theta = \sin f\tau$ in dimensionless variables) and the bottom wall temperature is kept at constant temperature T_0 ($\theta = 0$). Fig. 1(c) shows Case 2 for which the top wall temperature is kept at T_0 ($\theta = 0$) and the bottom wall temperature $T_0 + T_1 \sin \omega t$ ($\theta = \sin f\tau$).

The basic dimensionless governing equations for fluid consist of equation of continuity, momentum equations in the X- and Y-coordinates and energy equation as follows:

$$\nabla \cdot \mathbf{U} = 0, \tag{1}$$

$$\frac{\mathrm{D}\mathbf{U}}{\mathrm{D}\tau} = -\nabla P + \nabla^2 \mathbf{U} + Gr\theta, \tag{2}$$

$$\frac{\mathrm{D}\theta}{\mathrm{D}\tau} = \frac{1}{Pr}\nabla^2 \theta. \tag{3}$$

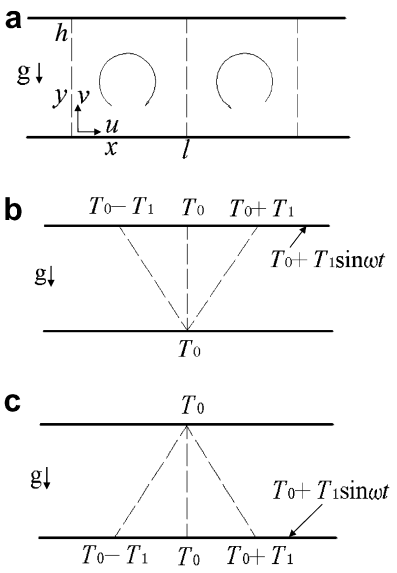

Fig. 1. Schematics of the system considered. (a) A roll cell between infinite horizontal flat walls. (b) Case 1. The top wall temperature is oscillated with $T_0 + T_1 \sin \omega t$, ($\theta = \sin f\tau$ in dimensionless temperature) and the bottom wall temperature is kept at T_0 constant ($\theta = 0$). (c) Case 2. The top wall temperature is kept at T_0 constant ($\theta = 0$) and the bottom wall temperature is oscillated with $T_0 + T_1 \sin \omega t$, ($\theta = \sin f\tau$).

Dimensionless initial and boundary conditions are as follows:

$$U = V = \theta = 0 \quad \text{at} \quad \tau = 0$$

$$U = \frac{\partial V}{\partial X} = 0, \quad \frac{\partial \theta}{\partial X} = 0 \quad \text{at } X = 0, 1$$

$$\begin{aligned}\text{Case 1}: U = V = \theta = 0 \quad & \text{at } Y = 0 \\ U = V = 0, \quad \theta = \sin f\tau \quad & \text{at } Y = 1 \\ \text{Case 2}: U = V = 0, \quad \theta = \sin f\tau \quad & \text{at } Y = 0 \\ U = V = \theta = 0 \quad & \text{at } Y = 1.\end{aligned} \tag{4}$$

The computation of the average Nusselt number needs some consideration, since the reference conduction state is not defined. For Case 1, we choose the reference conduction heat flux at the maximum temperature difference heated from below. This means the minimum temperature $T_0 - T_1$ at the top wall and T_0 at the bottom wall are chosen. Then conduction heat flux can be given as follows:

$$q_{\text{ref}} = k[T_0 - (T_0 - T_1)]/h = kT_1/h \tag{5}$$

For Case 2, the maximum temperature $T_0 + T_1$ is chosen for bottom wall and T_0 at the top wall and we get the reference conduction heat flux as follows:

$$q_{\text{ref}} = k[(T_0 + T_1) - T_0]/h = kT_1/h. \tag{6}$$

Then the reference heat flux is the same for two cases and we can compute the local Nusselt number as follows:

$$Nu_{\text{L}} = q_{\text{conv}}/q_{\text{ref}} = (-k\partial T/\partial y)/(kT_1/h) = -\partial\theta/\partial Y. \tag{7}$$

Then we can compute the average Nusselt number (geometrically averaged) as follows:

$$\begin{aligned} Nu_{\text{bottom}} &= -\frac{h}{l}\int_0^{\frac{l}{h}} \left.\frac{\partial\theta}{\partial Y}\right|_{Y=0} \mathrm{d}X, \\ Nu_{\text{top}} &= -\frac{h}{l}\int_0^{\frac{l}{h}} \left.\frac{\partial\theta}{\partial Y}\right|_{Y=1} \mathrm{d}X. \end{aligned} \tag{8}$$

The time-averaged Nusselt number is given by

$$\begin{aligned} \overline{Nu}_{\text{bottom}} &= -\frac{f}{2\pi}\cdot\frac{h}{l}\int_0^{2\pi/f}\int_0^{l/h} \left.\frac{\partial\theta}{\partial Y}\right|_{Y=0} \mathrm{d}X\mathrm{d}\tau, \\ \overline{Nu}_{\text{top}} &= -\frac{f}{2\pi}\cdot\frac{h}{l}\int_0^{2\pi/f}\int_0^{l/h} \left.\frac{\partial\theta}{\partial Y}\right|_{Y=1} \mathrm{d}X\mathrm{d}\tau. \end{aligned} \tag{9}$$

This definition agrees with that by Kalabin et al.

3. Computed results

3.1. The case of fluid layer 1:1

The above dimensionless equations are approximated with finite difference equations for a staggered, non-uniform grid system and solved with SIMPLER [10] algorithm numerically. The computational parameters are arbitrarily taken as $Gr = 4 \times 10^4$, $Pr = 1$, dimensionless oscillating frequency $f = 5\pi$ and the dimensionless oscillatory period $\tau_{\text{p}} = 2\pi/f = 0.4$. Grids are 51×51 and $\Delta\tau = 1 \times 10^{-4}$. Numerical convergence is presumed at each time instant when the following conditions are satisfied for U, V and θ shown as φ in the next equation where $\varepsilon = 10^{-5}$ and n is internal iteration number

$$\frac{\sum_{i,j}\left|\varphi_{i,j}^{n+1} - \varphi_{i,j}^{n}\right|}{\sum_{i,j}\left|\varphi_{i,j}^{n+1}\right|} \leqslant \varepsilon. \tag{10}$$

Numerical iterations should be continued until the standing oscillation are obtained after 5–10 periods with oscillating period $\tau_{\text{p}} = 2\pi/f$. Numerical computations are successfully carried out and the standing oscillatory temperature and flow field are obtained.

In Fig. 2(a), the oscillatory temperature of the top wall is indicated with the dashed line for Case 1 with sinusoidal temperature oscillation on the top wall with the constant average temperature on the bottom wall. Fig. 2(a) also shows transient response of the average Nusselt number, Nu_{top}, and it is shown with the solid line. Fig. 2(b) shows the average Nusselt number at the bottom wall, Nu_{bottom}. The oscillation period of the Nu_{top} is the same as that of the top wall temperature oscillation but the Nusselt number at the top wall has a peculiar sharp peak in each cycle. This peak occurs nearly at the time of the coldest temperature of the top wall. Otherwise, the response curve takes almost similar magnitude in positive and negative values.

In Fig. 2(b), Nu_{bottom}, shows oscillatory response but is different from that of Nu_{top} in its shape. Furthermore, Nu_{bottom} is positive at the most of time to suggest that the

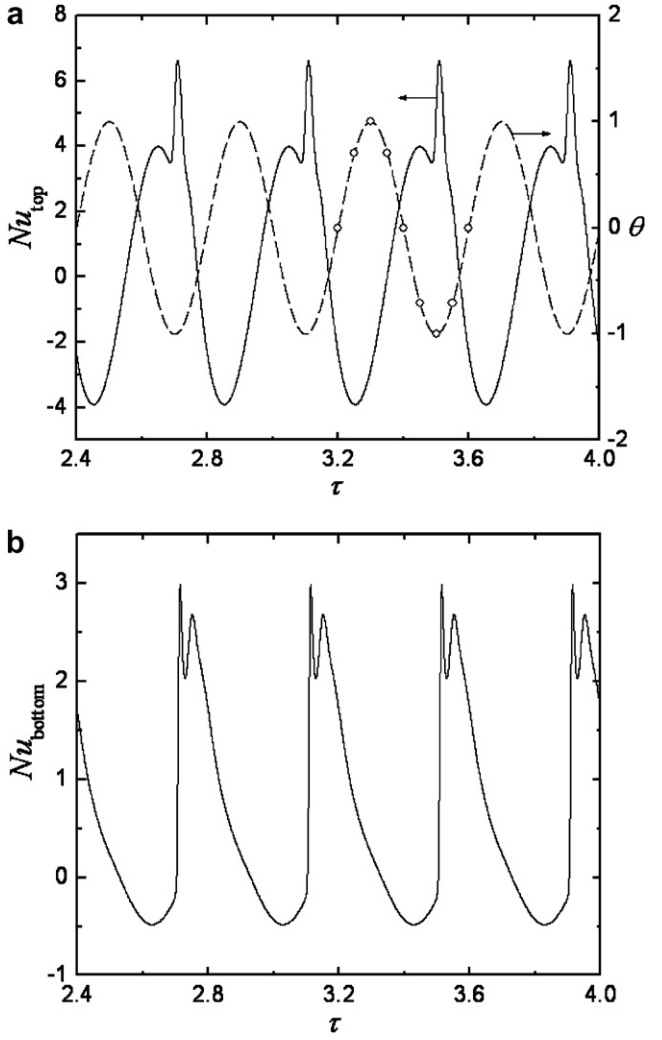

Fig. 2. Transient responses of the average Nusselt numbers for Case 1 at $Gr = 4 \times 10^4$, $Pr = 1$, $f = 5\pi$, $\tau_{\text{p}} = 0.4$. (a) Nu_{top}; (b) Nu_{bottom}.

total net heat flux is positive. Then, the time-averaged Nusselt number $\overline{Nu}$ is computed to have $\overline{Nu}_{top} = \overline{Nu}_{bottom} = 0.596$. This suggests that the net heat flux is from the bottom to the top wall even if the top wall temperature is sinusoidally oscillated and the net temperature difference is zero in a time-averaged sense. This characteristic agrees with the report by Kalabin et al. Then, let us observe the behavior more in detail.

Fig. 3 shows a series of computed contours of (a) isotherms and (b) stream function contours for $\tau = 3.2$–3.6. The time instants are every 0.05 which are marked on the top wall temperature curve in Fig. 2(a). The top wall temperature θ is indicated at the top wall in Fig. 3. By watching the change of isotherms with time for these nine time instants, we can see following. At $\tau = 3.2$, $\theta = 0$ and the top wall temperature starts to increase. At $\tau = 3.3$, $\theta = 1$, the top wall is at the maximum temperature. At $\tau = 3.4$, $\theta = 0$, temperature comes back to the average one. During this half cycle of the top wall temperature, the convection at $\tau = 3.2$ is suppressed and temperature stratification is established until $\tau = 3.45$. At $\tau = 3.5$, $\theta = -1$, the top wall temperature attains the minimum value and the strong downward flow occurs. This strong downward flow appears to correspond to the sharp peak in the Nu_{top} curve seen in Fig. 2(a). The peak in Nu_{bottom} curve occurs at almost the same time as Nu_{top} curve. At $\tau = 3.6$, $\theta = 0$, the one-cycle change in the top wall temperature ends.

Fig. 3(b) shows corresponding contours of stream function. Temperature rises from $\tau = 3.2$ and attains the maximum at $\tau = 3.3$. At $\tau = 3.25$ due to the heating effect from the top wall the convection is suppressed and we can see the weak reverse convection near the top wall. The temperature stratified weak convection area develops. At $\tau = 3.5$, the top wall temperature becomes the minimum, $\theta = -1$ which induces the bulk area convection as seen for $\tau = 3.5$–3.6.

In this way, the transient natural convection appears to represent a one-cycle rotation with a cycle change in the top wall temperature oscillation at least for the present combination of parameters.

Fig. 4 shows the counterparts for Case 2, the top wall temperature is kept at constant value of $\theta = 0$ and the bottom wall temperature sinusoidal, $\theta = \sin f\tau$. Otherwise the conditions are the same.

Fig. 4(a) shows the response of the average Nusselt number at the top wall for $\tau = 2.4$–4.0, four cycles. (b)

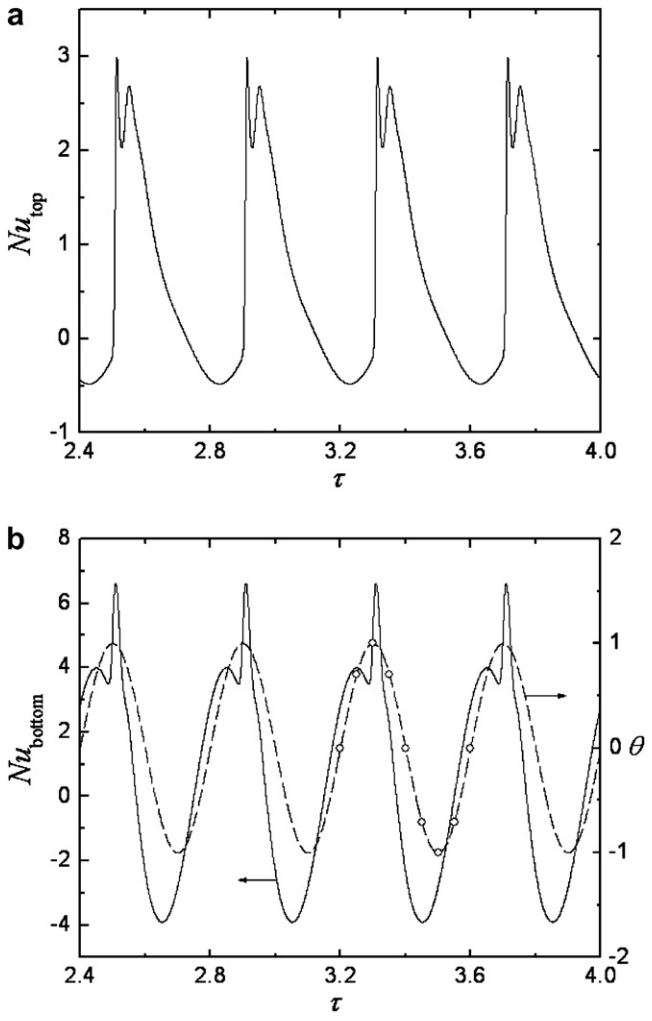

Fig. 4. Transient responses of the average Nusselt numbers for Case 2 at $Gr = 4 \times 10^4$, $Pr = 1$, $f = 5\pi$, $\tau_p = 0.4$. (a) Nu_{top}; (b) Nu_{bottom}.

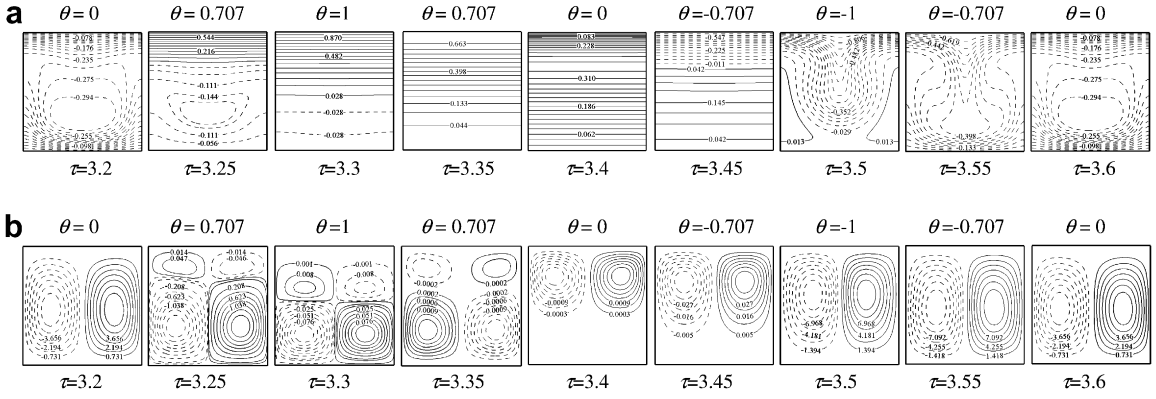

Fig. 3. A series of computed contours for $\tau = 3.2$–3.6 for Case 1 at $Gr = 4 \times 10^4$, $Pr = 1$, $f = 5\pi$, and $\tau_p = 0.4$. (a) Isothermal contours; (b) stream function contours.

shows that on the bottom wall. The average Nusselt number at the constant wall temperature, Nu_{top}, takes positive value for most of the time and takes similar shape as Fig. 2(b). At the bottom wall, with sinusoidal wall temperature, Nu_{bottom}, oscillates with time which is also similar shape as Fig. 2(a). Fig. 4(b) shows that the peak heat flux occurs almost at the same time as the peak in the bottom wall temperature (dashed curve). The time-averaged Nusselt number, however, take the same value $\overline{Nu}_{top} = \overline{Nu}_{bottom} = 0.596$. This means the time-averaged heat flux is again from the bottom wall to the top wall even if the bottom wall temperature oscillation gives net-zero temperature difference between the top and bottom wall, same as for Case 1.

Fig. 5(a) isothermal contours and (b) contours of stream function are the corresponding sequential pictures at the time instants marked on the curve of Fig. 4(b), at nine instants. This time, with the sinusoidal change in the bottom wall temperature, the development of temperature boundary layer can be seen for $\tau = 3.2$–3.4 with the positive temperature $\theta = 0 \to 1 \to 0$. Bulk convection is induced due to this for $\tau = 3.3$–3.4. For $\tau = 3.4$–3.6, $\theta = 0 \to -1 \to 0$ with negative temperature in the bottom wall and low temperature boundary layer develops for $\tau = 3.4$–3.6. For Case 2, the characteristics are quite similar to those for Case 1, though the contour maps are different each other.

Soong et al. [8] reported the phase lag between the average Nusselt number and the wall temperature and the similar occurs in Figs. 2(a) and 4(b).

Some other combinations of the Grashof number and the frequency are tested and the general characteristics of uni-directional heat transfer rate are similar.

3.2. The case of fluid layer 1:4

The main assumption for the present two-dimensional computation for roll cell is the computational area height:-width = 1:1. Thus another width of 4 is tested. For the case of fluid layer 1:4, the dimensionless initial and boundary conditions are

$$
\begin{aligned}
&U = V = \theta = 0 \qquad \text{at } \tau = 0\\
&U = \frac{\partial V}{\partial X} = 0, \quad \frac{\partial \theta}{\partial X} = 0 \quad \text{at } X = 0, 4\\
&\text{Case 1}: U = V = \theta = 0 \qquad \text{at } Y = 0\\
&\qquad\quad U = V = 0, \quad \theta = \sin f\tau \quad \text{at } Y = 1\\
&\text{Case 2}: U = V = 0, \quad \theta = \sin f\tau \quad \text{at } Y = 0\\
&\qquad\quad U = V = \theta = 0 \qquad \text{at } Y = 1.
\end{aligned}
\tag{11}
$$

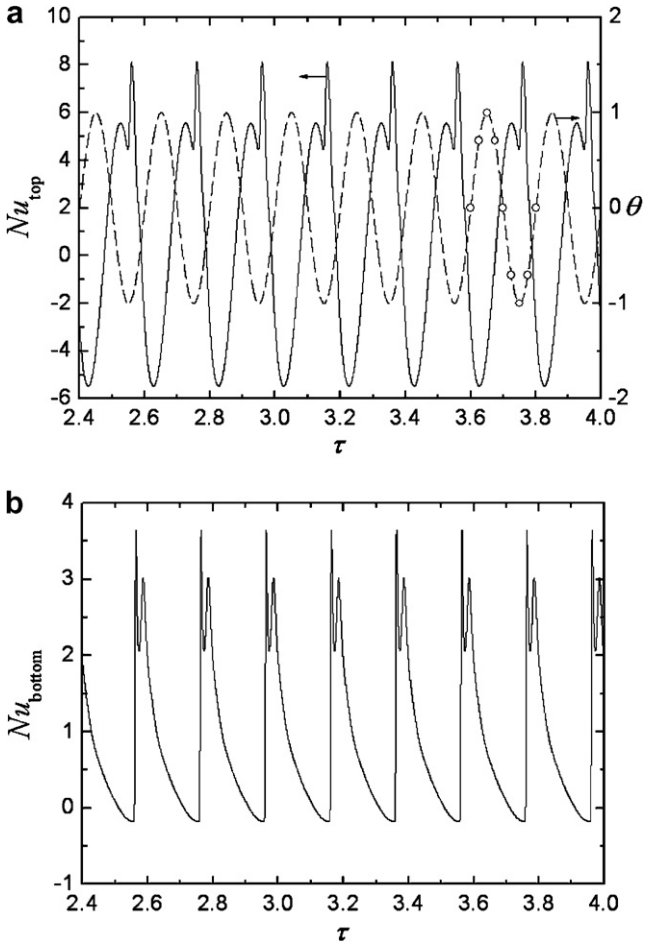

Fig. 6. Transient responses of the average Nusselt numbers for Case 1 for the computed area $l/h = 4$ at $Gr = 1 \times 10^5$, $Pr = 1$, $f = 10\pi$ and $\tau_p = 0.2$. (a) Nu_{top}; (b) Nu_{bottom}.

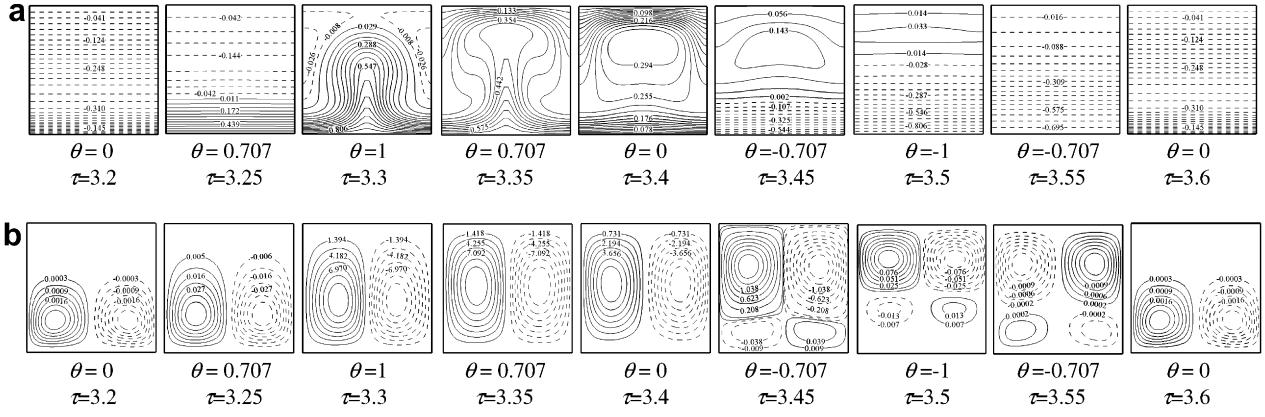

Fig. 5. A series of computed contours for $\tau = 3.2$–3.6 for Case 2 at $Gr = 4 \times 10^4$, $Pr = 1$, $f = 5\pi$, and $\tau_p = 0.4$. (a) Isothermal contours; (b) stream function contours.

Fig. 6 shows for Case 1 the transient responses of the average Nusselt number for the computed area for height:-width = 1:4 for $Gr = 10^5$, $f = 10\pi$ and $Pr = 1$. Again quite similar transient responses are obtained. The time-averaged Nusselt number is 0.844. For 1:1 fluid layer as before for the same conditions we obtained the time-averaged Nusselt number 0.834. Fig. 7 shows the detailed isotherms and stream function contours. There are mostly eight roll cells and the transient behavior appears to be quite similar to that obtained for 1:1 fluid layer even though at different Grashof number and frequency. These assure the previous computations for 1:1 layer also.

3.3. Computed result for one reference system

Herein we would like to present the computational result for natural convection in a square enclosure with sinusoidal wall temperature on the left-hand vertical side wall and a constant average temperature on the right-hand vertical side wall. The top and bottom horizontal walls are thermally adiabatic. This geometrical situation is the same as the bench-mark problem. Computational parameters are the same as the one presented in Figs. 2–5. Fig. 8(a) shows the transient responses of the average Nusselt number on the left-hand side wall, Nu_{left} and (b) the right-hand side wall, Nu_{right}. Nu_{left} is almost symmetrical in positive and negative magnitudes. Nu_{right} is also symmetrical in positive and negative, though its magnitude is about half of Nu_{left}. The time-averaged Nusselt numbers $\overline{Nu}_{\text{left}}$ and $\overline{Nu}_{\text{right}}$ are in the order of 10^{-7}. Considering the peak magnitude of Nu_{left} is 6 or so, these values are almost zero in net. This result represents that the time-averaged temperature difference in net-zero gives the net-zero heat transfer between two opposing vertical side walls. We present this sample com-

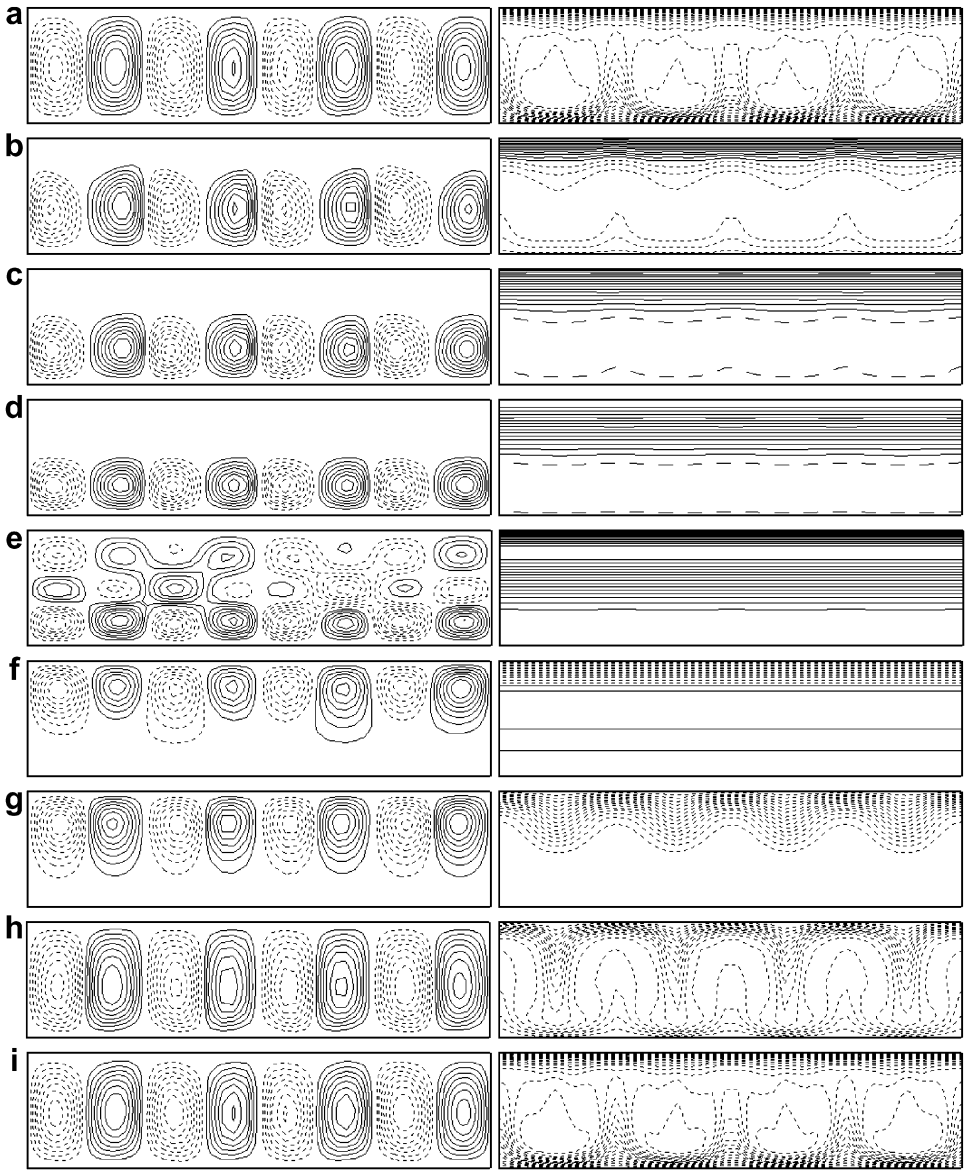

Fig. 7. A series of stream function contours (left) and isothermal contours (right) for $\tau = 3.6$–3.8 for Case 1 at $Gr = 1 \times 10^5$, $Pr = 1$, $f = 10\pi$ and $\tau_p = 0.2$. (a) $\tau = 3.6$; (b) $\tau = 3.625$; (c) $\tau = 3.65$; (d) $\tau = 3.675$; (e) $\tau = 3.7$; (f) $\tau = 3.725$; (g) $\tau = 3.75$; (h) $\tau = 3.775$; (i) $\tau = 3.8$.

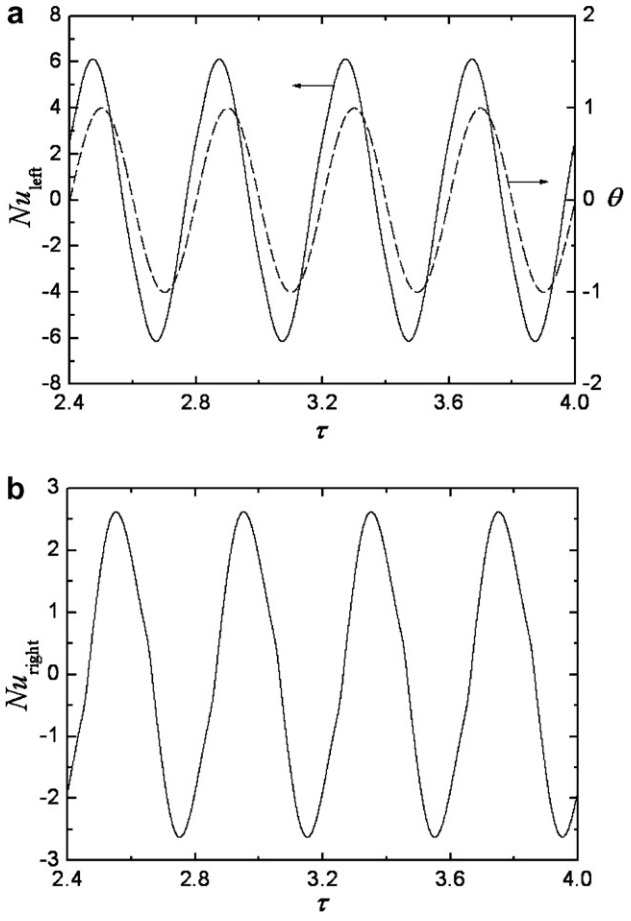

Fig. 8. Transient responses of the average Nusselt numbers over a vertical side wall of sinusoidal wall temperature on the left-hand side wall at $Gr = 4 \times 10^4$, $Pr = 1$, $f = 5\pi$ and $\tau_p = 0.4$. (a) Nu_{left}; (b) Nu_{right}.

putation to compare with the previous horizontal fluid layer. With using the same numerical code (with the revision for the boundary conditions only), the computation for a shallow horizontal fluid layer gives the uni-directional heat transfer from the bottom wall to the top wall even if the temperature difference is zero in time-averaged sense. This assures that the uni-directional heat transfer is not the outcome of our computer code.

3.4. Discussion

We obtained the above numerical results but experimental approach is necessary. Mantle et al. [11] reported the experimental heat flux with the oscillatory temperature variation over the bottom wall with net temperature difference all the time. The temperature oscillation does not increase the net heat flux when the temperature oscillation amplitude is less than 15% of the mean temperature difference but gives larger heat flux when the oscillation amplitude is more than 30% of the mean difference. Thus, actual outcome of the heat flux increase would depend on the oscillation amplitude and the oscillation frequency.

4. Conclusion

The two-dimensional numerical computations are carried out for the transient natural convection in a horizontal fluid layer with sinusoidal temperature difference either at the top or bottom wall with the average temperature at the opposing wall. The time-averaged temperature difference is zero between the top and bottom walls. The transient response in the average Nusselt number shows the oscillating behavior. The Nusselt number on the oscillating temperature wall gives positive and negative oscillation and the Nusselt number on the constant average temperature wall gives mostly positive values even if it oscillates in smaller magnitudes than that on the temperature oscillating wall. This gives always positive net heat flux from the bottom wall to the top wall uni-directionally. This is due to the bulk area convection induced near the maximum temperature difference with the top wall at the lower temperature and the bottom wall at the higher temperature. Similar results are obtained for two different frequencies of temperature oscillation, two different Grashof numbers and two different convection area widths. The reference computation is carried out for convection in a square cross sectional enclosure with the left-hand vertical side wall temperature sinusoidally oscillated and the right-hand vertical side wall temperature at the constant average value. This last example gives essentially net-zero magnitude of heat transfer both for $\overline{Nu}_{left}$ and $\overline{Nu}_{right}$. This assures the above outcome of the uni-directional heat flux is not due to our numerical system employed herein.

Acknowledgements

We would like to acknowledge financial support for this work provided by the National Natural Science Foundation of China (No.50521604). One of the authors, H. Ozoe, acknowledges the Foreign Expert Invitation Program of Xi'an Jiaotong University to serve the present research.

Appendix A

In the above computation, grid numbers 51×51 are employed based on the following results. Table 1 shows the time-averaged Nusselt number computed for two different combinations of Gr and oscillation frequencies. Four different grid numbers, 31×31, 41×41, 51×51 and 61×61 are tested. The time-averaged Nusselt number

Table 1
Effect of grids on the time-averaged Nusselt numbers for some cases ($Pr = 1$)

f	Gr	$\overline{Nu}$			
		31×31 grids	41×41 grids	51×51 grids	61×61 grids
3π	5×10^4	0.796	0.808	0.818	0.826
5π	1×10^5	1.054	1.061	1.074	1.083

agrees mostly each other and we employed 51×51 in the above computations for which the time-averaged Nusselt numbers are within 1% or less than those at 61×61.

References

[1] T.D. Foster, Stability of a homogeneous fluid cooled uniformly from above, Phys. Fluids 8 (1965) 1249–1257.
[2] T.D. Foster, Effect of boundary conditions on the onset of convection, Phys. Fluids 11 (1968) 1257–1262.
[3] S. Mitsumoto, H. Ueda, H. Ozoe, A laboratory experiment on the dynamics of the land and sea breezing, J. Atmos. Sci. 40 (1983) 1228–1240.
[4] H. Ueda, S. Komori, T. Miyazaki, H. Ozoe, Time-dependent thermal convection in a stably stratified fluid layer heated from below, Phys. Fluids 27 (1984) 2617–2623.
[5] M. Kazmierczak, Z. Chinoda, Buoyancy-driven flow in an enclosure with time periodic boundary conditions, Int. J. Heat Mass Transfer 35 (1992) 1507–1518.
[6] J.L. Lage, A. Bejan, The resonance of natural convection in an enclosure heated periodically from the side, Int. J. Heat Mass Transfer 36 (1993) 2027–2038.
[7] H.S. Kwak, J.M. Hyun, Natural convection in an enclosure having a vertical side wall with time-varying temperature, J. Fluid Mech. 329 (1996) 65–88.
[8] C.Y. Soong, P.Y. Tzeng, C.D. Hsieh, Numerical study of bottom-wall temperature modulation effects on thermal instability and oscillatory cellular convection in a rectangular enclosure, Int. J. Heat Mass Transfer 44 (2001) 3855–3868.
[9] E.V. Kalabin, M.V. Kanashina, P.T. Zubkov, Natural convective heat transfer in a square cavity with time varying side wall temperature, Numer. Heat Transfer A: Appl. 47 (2005) 621–631.
[10] S.V. Patankar, Numerical Heat Transfer and Fluid Flow, McGraw-Hill, New York, 1980.
[11] J. Mantle, M. Kazmierczak, B. Hiawy, The effect of temperature modulation on natural convection in a horizontal layer heated from below: high-Rayleigh-number experiments, ASME J. Heat Transfer 116 (1994) 614–620.